Texture Analysis and Synthesis using Angular Wavelet Frames

R. Venkateswara Rao, IIT Kanpur

Sumana Gupta, IIT Kanpur

Abstract- The paper describes a new method for texture analysis and synthesis using angular wavelet frames (AWF). The objective of using AWF is to improve the performance of existing wavelet based classification algorithms for textured images having dominant angular components, as well as the synthesis algorithms for textures with long range and non linear spatial correlation. The 2D AWF is constructed by frequency transformations of the prototype 1D perfect reconstruction filter bank (PRFB). Encouraging results have been obtained by this method.

1. INTRODUCTION

In recent years, the issue of texture analysis and synthesis has been extensively investigated. The methods based on discrete wavelet transform (DWT) and its variant the discrete wavelet frame (DWF) provide a precise and unifying framework for analysis and characterization of textures at different scales. However, as these methods decompose the frequency plane into four rectangular segments, the analysis of textures with dominant angular components is rather poor. In this paper we propose the construction of angular wavelet frames (AWF) to overcome this problem. We construct 2D AWF by using the combination of 2D circular and 2D angular transformed filters. The overall classification rate using the AWF method is higher than that of the DWT and DWF methods. This is because the AWF can capture the dominant angular components of the textures. For texture synthesis auto regressive (AR) image models have been largely used with some degree of success. The drawback of AR models is that it is sensitive to the choice of model order and the power spectra and auto correlation functions of the AR models do not always resemble those of original texture images. As a result there is considerable research interest in multiresolution/multi scale statistical image models [1-4] for texture synthesis.

The basic idea is to construct a complex model from a number of simpler models that require reduced computational cost. In this paper we also propose an angular wavelet-based statistical model for texture synthesis using AWF and AR model. The synthesis results demonstrated that the proposed model is superior to DWT method especially for textures containing non-linear and long-range correlation.

In section 2, we give the definition of the filter banks and explain the method of constructing 2D angular wavelet frames using frequency transformations. We discuss the angular wavelet-AR model applied to texture, in section 3. In section 4, we describe the experimental results obtained on "Broadtz" textures.

2. CONSTRUCTION OF AWF

In this section, we characterize the perfect reconstruction filter banks (PRFB) underlying the definition of the discrete wavelet transforms, used in this work. We start with the prototype filters h and g, which satisfy the condition

$$H(z)\widetilde{H}(z) + G(z)\widetilde{G}(z) = 1 \qquad (1)$$

where H (z) and G (z) are the z – transforms of the prototype filters h and g. These prototype filters are then used to generate, in an iterative fashion, a sequence of filters of increasing width (indexed by i)

$$H_{i+1}(z) = H(z^{2^i})H_i(z)$$
$$G_{i+1}(z) = G(z^{2^i})H_i(z), \quad (i=0,1,...,I-1) \qquad (2)$$

with the initial condition H_0 (z) = 1. It can be easily shown that such sequences of filters also satisfy the identity

$$H_i(e^{j\omega})\widetilde{H}_i(e^{j\omega}) + \sum_{k=1}^{i} G_k(e^{j\omega})\widetilde{G}_k(e^{j\omega}) = 1 \qquad (3)$$

and therefore, provide a full coverage of the frequency domain.

We use frequency transformation methods to construct a 2D filter from a 1D filter. 2D filters are constructed using circular and angular transformations on 1D filters. Consider the transform

$$H(\omega_1,\omega_2) = H(\omega)\big|_{\omega=T(\omega_1,\omega_2)} \qquad (4)$$

The two transformations used are:

$$T(\omega_1,\omega_2) = \sqrt{\omega_1^2 + \omega_2^2} \quad - circular\ transformation$$

$$= 2*\mathrm{atan}(\omega_2/\omega_1) \quad - angular\ transformation \qquad (5)$$

Frequency supports of the above transformations are shown in the Fig.1a.
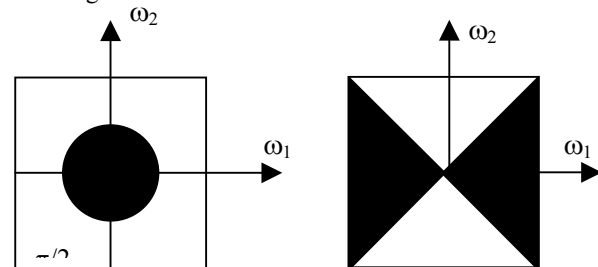

Fig.1. Frequency supports of Circular and Angular Transformations

2.1. Construction of 2D Angular Wavelet Frames

2.1.1. Decomposition at Level 1: To construct 2D angular wavelet frame based on 1D wavelet frame, we consider 1D PRFB filters $H(\omega)$ and $G(\omega)$. On applying the circular

and angular transformations described in Equation (5) we obtain four filters H_c, G_c, H_a and G_a.

$$H_c(\omega_1,\omega_2) = H(\omega)\big|_{\omega=\sqrt{\omega_1^2+\omega_2^2}}$$

$$G_c(\omega_1,\omega_2) = G(\omega)\big|_{\omega=\sqrt{\omega_1^2+\omega_2^2}}$$

$$H_a(\omega_1,\omega_2) = H(\omega)\big|_{\omega=2*a\tan(\omega_2/\omega_1)} \quad (6)$$

$$G_a(\omega_1,\omega_2) = G(\omega)\big|_{\omega=2*a\tan(\omega_2/\omega_1)}$$

where the subscript 'c' and 'a' denotes circular and angular transformations respectively. A useful wavelet frame can be constructed with the analysis filters

$$F_{hh} = H_cH_a;\ F_{hg} = H_cG_a;\ F_{gh} = G_cH_a;\ F_{gg} = G_cG_a; \quad (7)$$

At the synthesis end, the conjugate filters are constructed using conjugates of the 1D filters in similar steps. The principle of this decomposition is illustrated in Fig. 2. The whole system of filters acts as an identity operator, i.e., the analysis and synthesis filters constitute a perfect reconstruction filter bank.
Property: The 2D analysis filters constructed by circular and angular transformations of 1D PRFB along with their conjugates at the synthesis end constitute a perfect reconstruction filter bank [5].
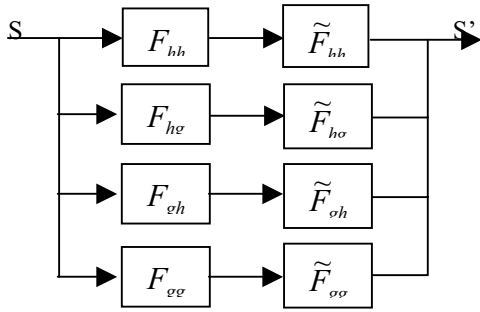

Fig. 2. One level Signal analysis and synthesis using the Angular Wavelet Frame decomposition

2.1.2. Decomposition at Higher Level- Consider the pyramidal decomposition where the low-low region is decomposed into four regions. The set of 1D-prototype filters, for the higher level of decomposition, is obtained using Equation (2). For level 2, we use H_2 and G_2 (i=1) to obtain 2D circular and angular transformed filters H_{2c}, G_{2c}, H_{2a} and G_{2a}. We consider the following combination of analysis filters:

$$F_{2hh} = H_{2c}\,H_{2a};\ F_{2hg} = H_{2c}\,G_{2a};$$
$$F_{2gh} = G_{2c}\,H_{2a};\ F_{2gg} = G_{2c}\,G_{2a}; \quad (8)$$

These four filters decompose the region supported by F_{hh} (HcHa) into four regions. They are used along with H_cG_a, G_cH_a and G_cG_a for the second level of decomposition. Using the pyramidal decomposition we obtain N = 1 + 3I (where I is the level of decomposition.) number of filters.
We can also decompose each of the other regions of the frequency plane into four regions. This is called tree structured decomposition method. Using Equation (2) we can get decomposition in the low-low frequency region only. In order to decompose the other regions, we should modify Equation (2). For the case of level 2, consider the following four equations:

$$H1H2(z) = H(z^2)H(z) \quad (9)$$

$$H1G2(z) = G(z^2)H(z) \quad (10)$$

$$G1H2(z) = H(z^2)G(z) \quad (11)$$

$$G1G2(z) = G(z^2)G(z) \quad (12)$$

The first two equations are the same as Equation (2) for i=1. Using circular and angular transformations on these four 1D filters we obtain 2D filters $H1H2_c$, $H1G2_c$, $G1H2_c$, $G1G2_c$, $H1H2_a$, $H1G2_a$, $G1H2_a$ and $G1G2_a$. Useful wavelet frame can be constructed by using appropriate combination of these 2D filters.

3. MODEL FOR TEXTURE SYNTHESIS

3.1. Angular wavelet-AR model

Let x be the texture having the wavelet coefficients as

$$x \sim \{w^1, w^2, \ldots, w^M, x^M\} \quad (13)$$

where w^m, m=1, 2,…, M are the angular wavelet coefficients at various levels. Each w^m contains three subsets w_1^m, w_2^m, w_3^m corresponding to low-high (LH), high-low (HL), and high-high (HH) components, and x^M contains low-low (LL) component at level M. Since x is completely determined from its angular wavelet coefficients, we can model x by modeling the wavelet coefficients independently.

We use parametric model which is an extension of AR model, and assume that the angular wavelet subbands are independent of each other. Hence, we can model each subband separately by using an AR model with the nonsymmetrical half plane (NSHP) neighborhood system shown in Fig.3. For example, a first order AR model can be used for low-low (LL) subband with

$$x_{i,j} = a_{0,1}x_{i,j-1} + a_{1,1}x_{i-1,j-1} + a_{1,0}x_{i-1,j} + a_{1,-1}x_{i-1,j+1} + \sigma^2 n_{i,j} \quad (14)$$

where $n_{i,j}$ is a zero-mean white Gaussian noise with variance σ^2. Similar first-order AR's can be used for the remaining angular wavelet subbands.
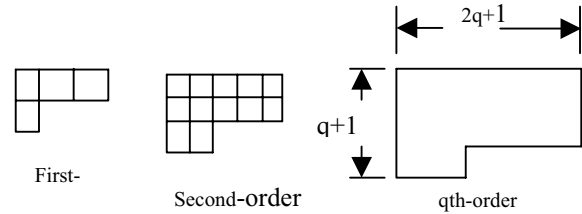

Fig.3.Nonsymmetrical half plane (NSHP) neighborhood systems

3.2. Parameter estimation and model synthesis

AR parameter estimation is done by solving Yule-Walker equations in each subband, while the model synthesis is done by generating an AR realization in each subband using equations like (14) and obtaining the synthesized texture from the modeled angular wavelet subbands.

4. EXPERIMENTAL RESULTS AND DISCUSSION

4.1. The Performance of Angular wavelet frames for texture synthesis

We performed the texture synthesis on several 'Brodatz' textures of size 128x128. We used 1-D 'db4' filters to construct the 2-D filters using frequency transformation

methods. Some results of texture synthesis using the second-level decomposition of the AWFs are shown in Fig.4. Along with the synthesis results, we also present the original prototype texture and the correlation plots for the original and synthesized textures respectively. We observe that the performance of the model using second-level decomposition of AWFs is better than that of the first-level decomposition of AWFs (Fig.4a). One can use still higher levels of decomposition to get better synthesis results, but the complexity of the model increases. In this work, we have used the second level decomposition of AWF. Generally, we have 4^I subbands in the decomposition, where I is the level of decomposition. For two level decomposition, we have 16 subbands. We decompose only those subbands, which contain significant information. The subbands to be decomposed are chosen by calculating the energy [6] of each subband and choosing those subbands with energy greater than 90% of the maximum energy contained in a subband. Hence if J is the number of subbands to be decomposed at second level, we have a total of 3J+4 subbands.

4.2. Comparison of the synthesis results using AWFs and using DWT

In this section, we present a comparison between the performances of the AR modeling of subbands using the AWFs with that of the Rectangular wavelets (DWT) for texture synthesis. In DWT, the decomposition is done in the low-low region only. If the texture image contains more edge information as shown in Fig.4, this will be in general present in the high-high region. In case of DWT, we cannot extract this information. In order to extract that information it is necessary that we decompose the region other than the low-low region as in AWF. Obviously, the performance of the texture synthesis using AWFs is far superior compared to that using DWT for the textures having more edge information. Fig.4b shows the synthesis results of an image of piecewise constant polygonal patches. The DWT is clearly unable to extract the edges, whereas the AWF has extracted them well. Fig.4c shows the checkerboard image, which is a binary image with only two intensity values. It contains non-linear correlation. The synthesis results using AWF satisfactory. The synthesis using DWT however is unstable, because of the abrupt change in the intensity level around each square in the image. In Fig.4d, the aluminum wire texture dominated by nonlinear correlation cannot be extracted by the DWT. However, the AWF is able to extract the brightness transitions remarkably well. Finally, our aim is to apply the proposed model on images that are structured and highly inhomogeneous. One such example is a face image, shown in Fig.4e. The synthesis using the proposed AWF performs satisfactorily. We observe that the images synthesized using DWT seems to contain local structures, but in a globally disorganized fashion. Fig.4f shows the synthesis results of the "herring bone" texture. Herringbone texture contains significant information in all directions. In order to extract information, it is necessary that we decompose all the sub bands at the second level decomposition of AWF. The synthesis result shown in Fig. 4f is satisfactory, but the complexity is high, as we have to model all 16 subbands at second level.

4.3   Performance of AWF for Texture Classification:
We performed classification experiments for 26 Bradatz textures. Images taken are of size 256x256. The sub images are obtained by filtering the texture images with 2D AWF. The variances of filtered images are chosen as component of feature vector. A comparison of overall classification rates of different methods is shown in Table 1.

5. CONCLUSIONS

In this paper, we propose an angular wavelet frame based multiresolution statistical model for texture synthesis. The 2D AWF is constructed by applying frequency transformations to the prototype filters of a 1D perfect reconstruction filter bank (PRFB). The basic idea is to construct a complex model from several simpler models. Our synthesis results demonstrate that the proposed model is superior to DWT method for textures dominated by nonlinear correlations. Very low order AR model is sufficient to model the subbands. This in turn requires a small number of AR parameters to represent the complete texture image. This is very useful in low bit rate applications. The classification results show that AWF is most suitable for textures with dominant angular components.

REFERENCES

[1] S. Lakshmanan, A. K. Jain, and Y. Zhong, "*Multi-resolution image representation using Markov random fields*", in Proc. ICIP'94, Austin, TX, vol. I, Nov. 13-16, 1994, pp. 855-860.

[2] T. W. Ryan, L. D. Sanders, and H. D. Fisher, "W*avelet-domain texture modeling for image compression*", in Proc. ICIP'94, Austin, TX, vol.II, Nov. 13-16, 1994, pp. 380-384 .

[3] J. M. Francos, A. Z. Meiri, and B. Porat, "*A unified texture model based on a 2-D Wold-like decomposition*", IEEE Trans. Signal Processing, vol. 41, Aug. 1993, pp. 2665-2678.

[4] J. Zhang, D. Wang, and Q. N. Tran, "*A wavelet-based multiresolution statistical model for texture*", IEEE Trans. Image Processing, vol. 7, Nov. 1998, pp. 1621-1627.

[5] K. Murali Mohan, "*Texture classification and segmentation using angular wavelet frames",* M.Tech Thesis, 2002, Department of EE, IIT Kanpur.

[6] Tianhorng chang and C. C. Jay Kuo, "*Texture analysis and classification with Tree-structured wavelet transform*", IEEE Trans. Image Processing, vol.2, No.4, Oct. 1993 , pp. 429-441.

Table 1: Comparison of Classification Rates (window   size 32*32)

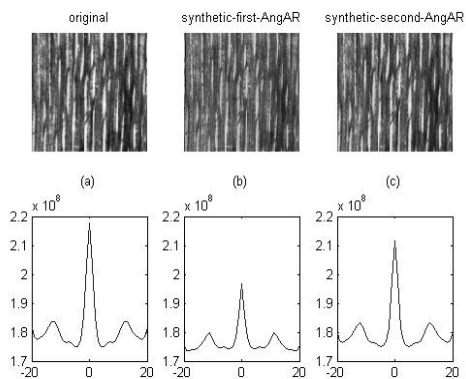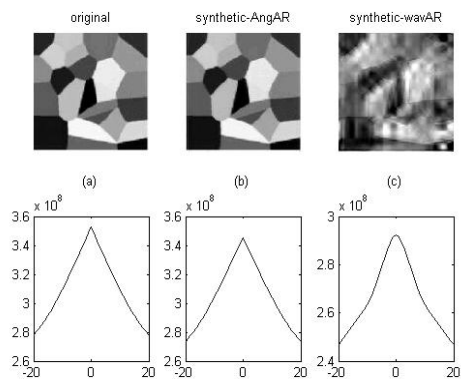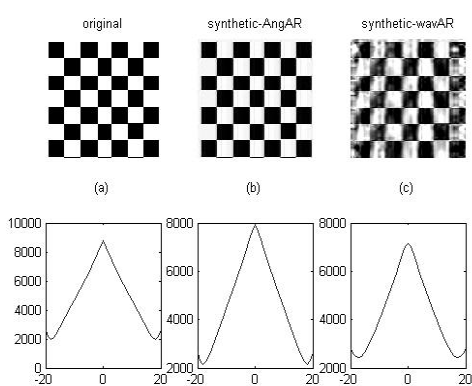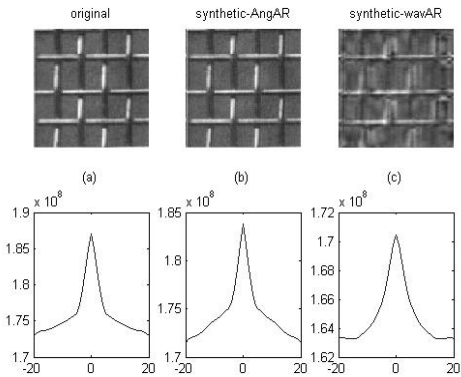| Method	DWT	DWF	AWF
Level 1-4 sub images	91.93%	96.48%	98.14%
Level 2-7 sub images	95.44%	98.83%	100.00%

Fig. 4a

Fig. 4b
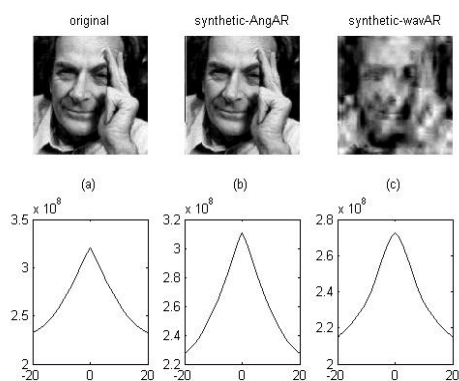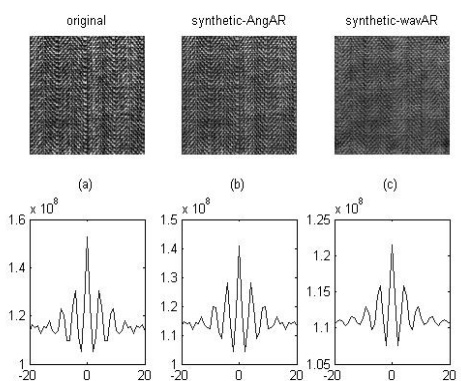

Fig. 4c

Fig. 4d

Fig. 4e

Fig. 4f

Fig. 4. Synthesis results of (a) D76 (b) Polygonal patches (c) Checker board (d) Aluminum wire (e) Face of a man (f) Herringbone textures, shown as

| 1 | 2 | 3 |
| 4 | 5 | 6 |

(1) Original texture (2) Synthesized using AWF (3) Synthesized using DWT (4),(5), and (6) Correlation plots of textures in (1), (2), and (3) respectively.